Mon. Not. R. Astron. Soc. **354,** 1133–1140 (2004) doi:10.1111/j.1365-2966.2004.08272.x

A laboratory survey of the thermal desorption of astrophysically relevant molecules

Mark P. Collings,[1⋆] Mark A. Anderson,[1] Rui Chen,[1] John W. Dever,[1] Serena Viti,[2⋆] David A. Williams[2] and Martin R. S. McCoustra[1⋆]

[1]*School of Chemistry, University of Nottingham, University Park, Nottingham NG7 2RD*
[2]*Department of Physics and Astronomy, University College London, Gower Street, London WC1E 6BT*

Accepted 2004 August 1. Received 2004 July 16; in original form 2004 March 29

ABSTRACT

The thermal desorption characteristics of 16 astrophysically relevant species from laboratory analogues of the icy mantles on interstellar dust grains have been surveyed in an extensive set of preliminary temperature programmed desorption experiments. The species can be separated into three categories based on behaviour. Water-like species have a single relevant desorption coincident with water. CO-like species show the volcano desorption and co-desorption of trapped molecules, monolayer desorption from the surface of water ice, and multilayer desorption if initially present in sufficient abundance in an outer layer separated from the water ice. Intermediate species show the two desorptions of trapped molecules, and may show a small monolayer desorption for molecules small enough to have a limited ability to diffuse through the structure of porous amorphous water ice. Methods by which the results obtained under laboratory conditions can be adapted for astrophysical situations are discussed.

Key words: astrochemistry – molecular processes – methods: laboratory – stars: formation – ISM: molecules.

1 INTRODUCTION

Hot cores are compact clumps within molecular clouds; they have high density and warm temperature and are found in the vicinity of young massive stars. They have a characteristically rich chemistry that provides evidence for the sublimation of grain mantle ices. Because the 'turn on' time of such massive stars is brief on astronomical time-scales, models of the hot-core chemistry have conventionally treated the sublimation process as instantaneous. In a recent publication, Viti & Williams (1999) described a hot-core model in which grains were warmed with a finite heating rate; they applied simple desorption kinetics, allowing species to sublime at varying temperatures. A significant chemical dependence on heating rate was found, suggesting that from observations of hot-core chemistry it may be possible to determine the age of the hot core and the rise time of the hot massive star. Possible evidence of non-instantaneous sublimation comes from the observational studies of Pratap, Megeath & Bergin (1999) and Hofner, Wiesemeyer & Henning (2001). However, before hot-core models can be used in such a diagnostic manner, a thorough understanding of the desorption processes of icy mantles must be established and applied.

In a series of recent publications, we have measured the desorption kinetics of carbon monoxide (CO) from solid films on the surface of water (H_2O) ice films, and from intimate mixtures with water ice (Collings et al. 2002, 2003a). Based on these laboratory experiments, a kinetic model that allows prediction of the desorption characteristics of CO under astrophysical conditions has been developed (Collings et al. 2003b). The behaviour of CO was found to be much more complex than the models typically applied at present would suggest. Water ice is able to trap and retain CO to much higher temperatures than is suggested by the strength of CO adsorption to CO (i.e. CO sublimation energy) and H_2O surfaces. The mechanism of this CO entrapment is an irreversible phase change in the water ice from a highly porous amorphous structure to a less porous amorphous phase. The change seals off pores from the surface and prevents CO adsorbed within these pores from escaping to the gas phase. Other volatile molecules of astrophysical relevance, including oxygen (O_2), nitrogen (N_2) and methane (CH_4), have been shown to behave with similar trapping behaviour to CO (Ayotte et al. 2001; Horimoto, Kato & Kawai 2002). When the low-porosity amorphous water phase crystallizes, trapped molecules are released in a desorption process, which is sometimes referred to as a molecular volcano (Smith et al. 1997). A fraction of the trapped molecules is retained until the crystalline water film itself desorbs. The intensity of this co-desorption peak is dependent on the thickness of the water film (Collings et al. 2003b).

By 'trapping' we refer to the physical containment of a species within the structure of the water film such that breaking of the bond between the adsorbate and the water surface is not a dominant

⋆E-mail: pczmpc@unix.ccc.nottingham.ac.uk (MPC); sv@star.ucl.ac.uk (SV); martin.mccoustra@nottingham.ac.uk (MRSM)

process in determining the temperature at which desorption occurs. Therefore, by our definition molecules adsorbed on internal pore surfaces are not 'trapped' if there remains a pathway to the external surface of the water film. Trapping of various molecules when co-deposited in intimate mixtures with water has been previously reported by numerous authors. The trapping of species such as CO, CO_2, CH_4 and NH_3 has been studied using infrared spectroscopy alone (Sandford et al. 1988; Sandford & Allamandola 1988; Schmitt, Grim & Greenberg 1988; Schmitt, Greenberg & Grim 1989; Sandford & Allamandola 1990). Kouchi (1990) examined CO trapping in mixtures with water using a combination of vapour pressure studies and electron diffraction, while Hudson & Donn (1991) investigated the same system in a combined temperature programmed desorption (TPD) and infrared spectroscopy study. Using TPD, Bar-Nun and coworkers have observed trapping in water films of a range of species, including N_2, CO and CO_2, during annealing of both co-deposited mixtures and sequentially adsorbed films (Bar-Nun et al. 1985; Laufer, Kochavi & Bar-Nun 1987; Notesco & Bar-Nun 1996; Notesco, Bar-Nun & Owen 2003).

There is some evidence supporting the trapping of CO and other molecules within porous amorphous water ice in astrophysical environments. Jørgensen, Schöier & van Dishoeck (2002) found that the differences in the CO abundances in class 0 and class I low-mass young stellar objects are consistent with CO trapping. Schöier et al. (2002) suggest that many of the observational traits towards IRAS 16293–2422 are consistent with CO trapping. Nomura & Millar (2004) have modelled the radial profiles of molecular abundances in a hot core considering trapping of many species within porous water ice, and suggest that detailed observations of the radial profiles of molecular abundances in hot cores may be able to constrain the fraction of trapping in these environments.

In this communication, we present the results of a preliminary survey of the desorption behaviour of a range of astrophysically relevant species during thermal processing. To study the desorption kinetics of each species in detail will require many years of research. The purpose of the research presented here is to provide a set of realistic first approximations describing desorption processes from porous water ice, which will suffice until more rigorous data become available, for use in astrophysical applications. These results have been applied to the chemical modelling of hot cores described in an accompanying paper (Viti et al. 2004).

2 EXPERIMENTAL

2.1 Choice of molecules for survey

From the list of important species modelled in the chemistry of hot cores (Viti & Williams 1999), we have chosen a range of species that are commonly available in chemical laboratories and that can be conveniently and safely handled without modification to our equipment. Ions, and radicals such as SO, are unstable under laboratory conditions, and therefore are not suitable for experimentation with our apparatus. Metal (in the true chemical sense) species such as magnesium have not been included, but represent an interesting possibility for future research.

The following chemicals have been used in this research. The gases nitrogen (N_2 – 99.999 per cent, BOC), oxygen (O_2 – 99.999 per cent, BOC), carbon monoxide (CO – 99.3 per cent, BOC), methane (CH_4 – 99 per cent, BOC), deuterated ethene (C_2D_4 – 99 per cent D, CDN), sulphur dioxide (SO_2 – 99.9 per cent, Aldrich), carbonyl sulphide (OCS – 99 per cent, Matheson), ammonia (NH_3 – 99.99 per cent, Aldrich) and hydrogen sulphide (H_2S – 99.6 per cent, BDH) were used without further purification. Deuterated ethene, C_2D_4, was used rather than C_2H_4 due to availability. Ethyne gas (C_2H_2 – 99.6 per cent, Air Products) was freeze-pump-thawed in an acetone–liquid-nitrogen slurry to remove contaminant acetone. The liquids methanol (CH_3OH – analytical grade, Fischer), methanoic acid (HCOOH – 96 per cent, Aldrich), acetonitrile (CH_3CN – 99.5 per cent, Aldrich), carbon disulphide (CS_2 – 95 per cent, Timster) and water (deionized) were purified by repeated freeze-pump-thaw cycles. Carbon dioxide (CO_2) was obtained as dry ice (BOC), and purified by repeated bulb-to-bulb distillations.

2.2 Apparatus and techniques

The apparatus used in this research has been described in detail elsewhere (Fraser, Collings & McCoustra 2002), therefore only a brief description of the experiment is necessary. All experiments were performed in an ultrahigh vacuum chamber with a base pressure of 1×10^{-10} mbar. The deposition of each species is measured as exposure, in units of L_m (1×10^{-6} mbar s), with the pressure determined by an ionization gauge. Each species was introduced to the chamber as a pure gas, effusively directed at the sample substrate by glass dosing lines from a distance of roughly 75 mm. Exposures of 100 L_m of water, and 5 L_m of all other species were used, and the temperature of the substrate was 8–10 K for all depositions. When water and a second species were simultaneously adsorbed (co-deposited), they were introduced via separate dosers, rather than from a pre-prepared gaseous mixture, using a pre-calibrated mass spectrometer signal to measure the partial pressure of one species. The substrate upon which the gases were adsorbed was a copper plate covered by a film of polycrystalline gold. TPD experiments were performed by heating the substrate at an approximately constant rate of 0.08 K s^{-1}, and measuring the rate of desorption of multiple species with a quadrupole mass spectrometer.

3 RESULTS

The desorption experiments are divided into three sets. In the first set, shown in Fig. 1, each species was deposited as a pure film on to the gold substrate. The 5-L_m exposure is sufficient for multilayer (solid) growth of each species. Fig. 2 shows the TPD traces of each species when deposited on to a pre-existing film of H_2O. At 10 K and below, the adsorption of all of these species is ballistic – the incident molecules can undergo only minimal rearrangement, and remain adsorbed essentially at the site of their collision with the surface. Therefore, this sequential adsorption procedure results in a layered ice film. In the third set of experiments, shown in Fig. 3, each species was co-deposited with water to form an intimate mixture. Experiments were also performed in each set using CH_4, NO and C_2D_4. However, poor-quality data were obtained for these three species in the sequential and co-deposition experiments, and the results have not been reproduced in Figs 2 and 3. The temperature of the radiation shield surrounding the cold finger of the cryostat is just cold enough to allow adsorption of these three species during deposition. During the TPD experiment, the radiation shield is warmed slightly, causing a broad desorption feature to appear in the TPD trace. In future experiments, this problem can be eliminated by installing a heater on the cryoshield to raise its temperature above the critical range during deposition. From these sets of experiments, all of these species can be assigned to one of three categories, based on their desorption behaviour.

Category 1 – CO-like species. The most volatile species include N_2, O_2, CO and CH_4. Their TPD traces from the pure film (Fig. 1)

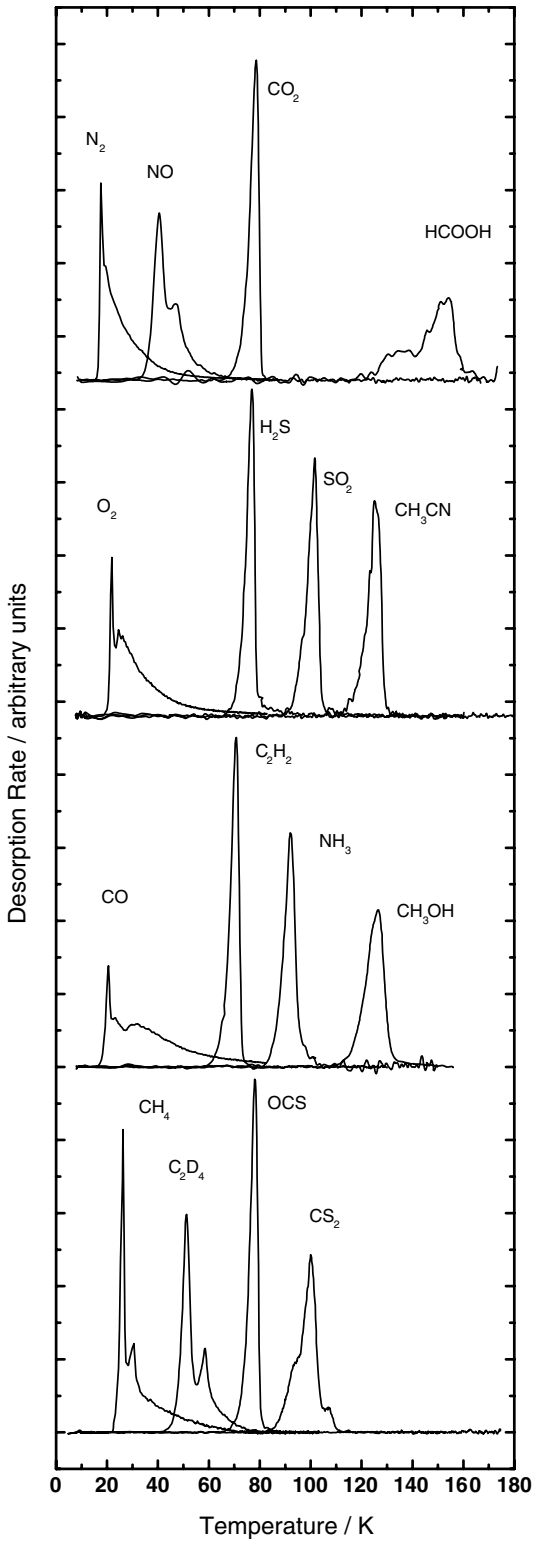

Figure 1. TPD traces of various species (5-L_m exposure) deposited on to a bare gold substrate. Each trace has been arbitrarily scaled such that the total desorption yield is equal. Traces are offset in four groups for clarity.

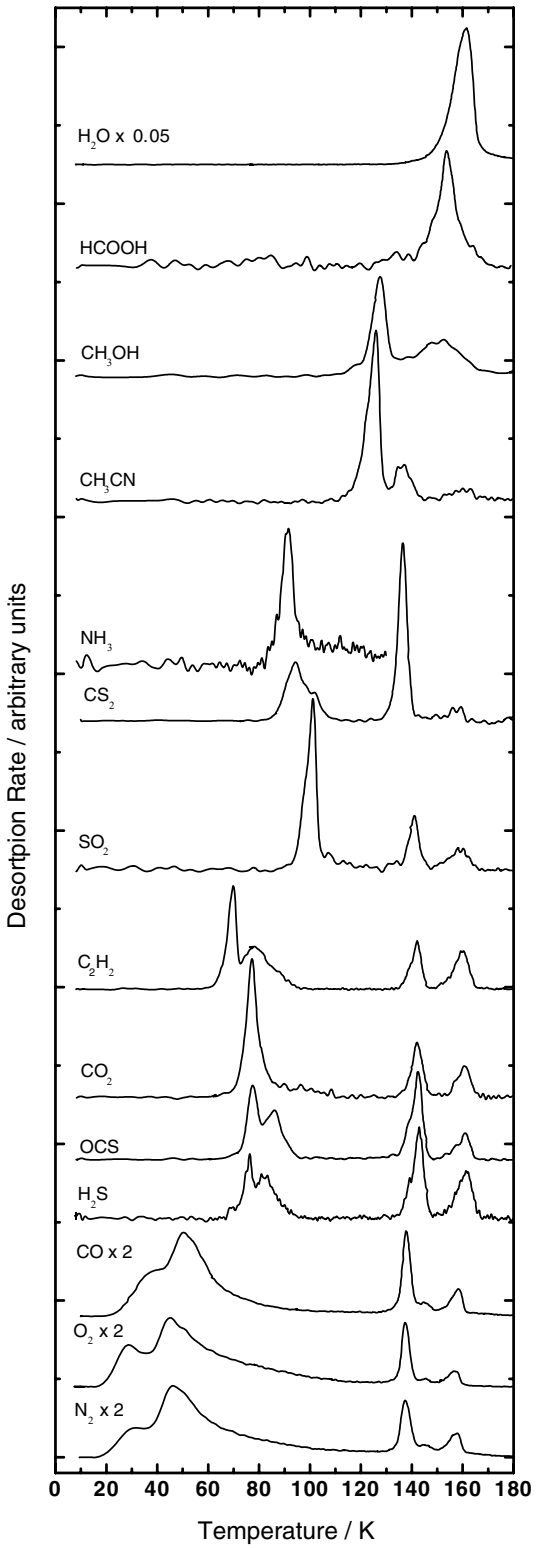

Figure 2. TPD traces of various species (5-L_m exposure) deposited on to a pre-adsorbed H_2O film (100 L_m). Traces are offset for clarity. Each trace has been arbitrarily scaled such that the total desorption yield is proportional to the exposure. The CO, O_2 and N_2 traces have been further scaled by a factor of 2 for clarity. The H_2O trace for each experiment was the same within experimental error. Therefore, only a single H_2O trace is shown, and this has been further scaled by a factor of 0.05 for clarity.

each show two peaks, corresponding to desorption of multilayer (solid) and monolayer (surface bound) molecules. The desorption temperatures compare well with previously published TPD experiments (Yoshinobu & Kawai 1996; Ramseyer et al. 1998; Dohnálek

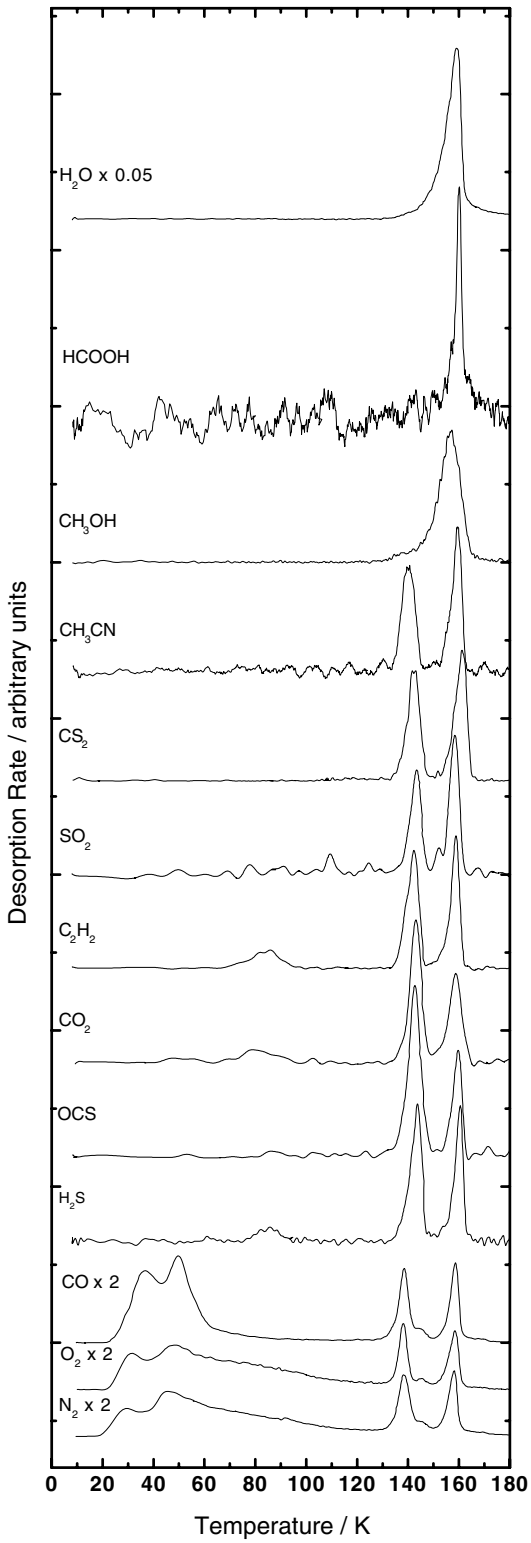

Figure 3. TPD traces of various species (5-L_m exposure) co-deposited with H_2O (100 L_m). Traces are offset for clarity. Each trace has been scaled arbitrarily as in Fig. 2. The H_2O trace for each experiment was the same within experimental error. Therefore, only a single H_2O trace is shown.

et al. 2001; Fraser et al. 2001). The TPD traces for CO, N_2, O_2 and CH_4 desorbing from layered systems also show good agreement with previously published data (Ayotte et al. 2001; Collings et al. 2003a,b). Multilayer peaks are absent from the desorption trace in each case. Although two peaks are observed in the broad desorption in the 20–60 K range for each species, the lower-temperature peak is in each case at too high a temperature to result from desorption of the solid species, and monolayer desorption accounts for all of the desorption in this range. The origin of the two-peak structure is not fully understood at present. We have previously found that solid CO overlayers will diffuse into the porous structure of water (Collings et al. 2003a). This diffusion process commences at temperatures lower than the desorption of multilayers, so if a slow heating rate is applied (as will be the case in astrophysical environments), diffusion of the solid CO overlayer into the water film will continue until the solid CO is exhausted or the water film is saturated with CO. The TPD trace for CO shown in Fig. 2 is consistent with our previously published data, and the traces for O_2, N_2 (Fig. 2) and CH_4 (not shown) demonstrate that rapid diffusion of solid overlayers into the ice also occurs for these species. Desorption features are also present at 140 K and 160 K corresponding to the volcano desorption and co-desorption processes of trapped molecules. The TPD traces of these species desorbing from co-deposited mixtures with H_2O (Fig. 3) show a strong similarity to those of the sequentially deposited experiments, showing both monolayer desorption features and the volcano desorption and co-desorption of trapped molecules. This demonstrates that the initial overlayers formed in the sequential deposition experiments are thoroughly dispersed through the ice film before desorption commences.

Category 2 – water-like species. In contrast to the CO-like molecules, NH_3, CH_3OH and HCOOH have desorption characteristics similar to those of water. Desorbing from the gold substrate, NH_3 and CH_3OH show only a single peak corresponding to multilayer desorption. This indicates that molecules are more strongly bound to neighbouring molecules in the film than they are to the gold surface, hence the monolayer desorption feature is suppressed by the growth of multilayers. The TPD trace for solid HCOOH is more complex. The two-peak structure suggests that HCOOH may undergo some sort of phase change at about 140 K. The crystallization of H_2O can be evident in TPD experiments where the heating rate is more rapid than applied here (Smith et al. 1997). Amorphous water ice has a higher vapour pressure than crystalline ice, so sublimes more rapidly. As a result, during TPD experiments, the desorption rate may increase with temperature, then decrease as amorphous water crystallizes, and increase again as crystalline water desorbs, giving a two-peak structure not dissimilar to that observed in Fig. 1 for HCOOH desorption. Multilayer desorption peaks are also clearly observed for NH_3 and CH_3OH desorbing from the surface of the water-ice layer (Fig. 2). Unlike the volatile species, NH_3 and CH_3OH are unable to diffuse into the porous structure of the water ice, so the solid film initially deposited largely remains in place during the TPD experiment. CH_3OH displays a second peak, coincident with H_2O desorption which can be attributed to desorption of monolayer molecules directly from the ice surface. This indicates that CH_3OH molecules bind more strongly to water molecules than to other CH_3OH molecules. It is likely that NH_3 behaves in the same way as CH_3OH. However, the dominant mass fragments of NH_3 at 17 and 16 amu are overwhelmed by signals from the more abundant H_2O molecules. While it is theoretically possible to subtract the component due to OH^+ from the total signal at 17 amu to leave the signal due to NH_3^+, our data quality was insufficient to make this a reliable analysis procedure. We are therefore unable to detect NH_3 desorption when it is coincident with H_2O desorption. However, the NH_3 multilayer peak observed from the ice surface is smaller than that for the equivalent dose on to the bare gold substrate, and low exposures of NH_3 on the ice

surface produced no detectable NH_3 desorption (not shown). These observations support our belief that monolayer NH_3 is desorbed coincidentally with H_2O. The two-peak structure of HCOOH multilayer desorption is absent when it desorbs from the ice surface. The single desorption peak is also nearly coincident with the H_2O desorption. When deposited as a mixture with H_2O, the HCOOH desorption peak is sharp and occurs at a slightly higher temperature than the maximum in the H_2O desorption (Fig. 3). This indicates that the HCOOH–H_2O interaction is stronger than the H_2O–H_2O and HCOOH–HCOOH interactions. CH_3OH desorption from the mixture shows a single peak coincident with H_2O desorption, and from the lack of any detected NH_3 desorption, it is assumed that the co-deposited NH_3 also desorbs coincidentally with water. There is no evidence in any of the experiments with these three species of their release in a volcano desorption. The strength of their interaction with H_2O means that they are retained in the ice film until the water desorbs.

Category 3 – intermediate species. The species H_2S, OCS, CO_2, C_2H_2, SO_2, CS_2 and CH_3CN display behaviour in between the CO-like and water-like species, and are categorized as 'intermediate'. The desorption traces of each from pure solid (Fig. 1) all show a single desorption feature. The CS_2 peak has additional structure to the low-temperature side of the maximum, again suggesting the possibility of a phase change. The small shoulder on the high-temperature side of its peak maximum, however, is known to be an artefact. When desorbing from a sequentially deposited layered ice (Fig. 2), a volcano desorption and co-desorption peak is evident for each of the species, indicating that all are trapped in the water ice to some extent. However, all of the species also show a multilayer desorption. Thus, the ability of these species to diffuse into the porous structure of the water film at temperatures low enough for trapping to occur is much more limited than for the CO-like species. No evidence of a monolayer desorption peak is evident for CO_2 and SO_2, indicating that these species are more strongly bound to themselves than to the water-ice surface. As on the bare substrate surface, the monolayer desorption process is suppressed by the presence of multilayers of CO_2 and SO_2. The rest of these intermediate species show a monolayer desorption feature, although for CS_2 it is not clearly resolved from the multilayer desorption, and for CH_3CN, it partially overlaps with the volcano peak. As expected, there is no evidence of any multilayer desorption peaks for any of the intermediate species when they desorb from intimate mixtures with water (Fig. 3). Volcano and co-desorption peaks are present in all cases. Despite the significant variation in observed volatility (Fig. 1) and strength of adsorption on ice (Fig. 2), the ratio of intensity for these two peaks is very similar for all of the intermediate and CO-like species. Clearly, the characteristics of the water-ice film control the release of trapped species. In contrast to the CO-like species, the intermediate species, when co-deposited with water, show only a very limited ability to diffuse though the water-ice structure – only C_2H_2 and H_2S (and perhaps CO_2) show evidence of a monolayer desorption peak. Although OCS has a similar adsorption strength to the water ice, it is a larger molecule and does not escape at monolayer desorption temperatures. Therefore, the size of the molecule appears to be important in limiting diffusion within the water-ice structure.

In addition to the poor-quality data obtained for NO and C_2D_4, their behaviour shows that they are on the border between the CO-like and intermediate categories. Their desorption profiles from the gold surface (Fig. 1) resemble those of the CO-like species, showing both multilayer and monolayer desorptions. Like the intermediate species, NO appears to retain a small multilayer peak when desorbing from the ice surface (not shown), and its ability to diffuse out of a co-deposited mixture with water to desorb in monolayer peaks (not shown) is more limited than that of the CO-like species. C_2D_4 does not show a multilayer desorption from the ice surface (not shown), but also shows only a limited ability to diffuse through water ice when co-deposited (not shown). Given the sizes of these molecules relative to those in the CO-like and intermediate categories, and the fact that collapse of the high-porosity phase of amorphous water ice will occur at lower temperature in astrophysical environments than in laboratory studies (Collings et al. 2003b), we will classify NO as CO-like and C_2H_4 as intermediate.

4 DISCUSSION

The desorption characteristics of most of the species analysed show strong dependence on the deposition technique (pure; sequentially deposited; co-deposited). It is therefore essential to consider which experimental deposition technique best reproduces ices formed in astrophysical environments.

Water ice is thought to be predominantly formed reactively on the surface of interstellar dust grains, by reaction of atomic hydrogen and oxygen (Jones & Williams 1984; O'Neill & Williams 1999). Similarly, other hydrogenated species are also believed to be formed in this manner by reaction of abundant H atoms with C, O, N and S atoms (Allamandola et al. 1999). Thus hydrogenated species, such as CH_4, C_2H_2, C_2H_4, CH_3OH, HCOOH, CH_3CN, NH_3 and H_2S, are likely to be found dilutely mixed in an ice layer dominated by water, and are therefore best represented by the co-deposited mixtures. NO is thought to be formed by energetic processing of such ices. By contrast, diatomic molecules such as CO, N_2 and O_2 are believed to be formed in gas-phase reactions, and are present in astrophysical ices due to 'freeze out'; i.e. adsorption from the gas phase on to cold surfaces. A model of ice mantle structure commonly applied is the 'onion layered' model, in which water and the other hydrogenated species form an inner layer of hydrogen bonded (polar) ice, surrounded by an outer layer of CO-, O_2- and N_2-rich ice in which the bonding is dominated by van der Waals interactions (apolar ice). The sequential deposition experiments are therefore the best representation of the desorption of the simple diatomic species. Observational evidence suggests that CO_2 and OCS are commonly found in the presence of water and other hydrogenated species such as methanol (Palumbo, Geballe & Tielens 1997; Dartois et al. 1999). Therefore, their behaviour should be best represented by co-deposition experiments. While there is no observational evidence to suggest what sort of ice environment other non-hydrogenated polyatomic molecules such as CS_2 and SO_2 might exist in, it is likely that they are formed by similar formation mechanisms to those of CO_2 and OCS, and therefore by analogy are also best represented by co-deposition experiments.

Once the appropriate deposition procedure for each species is recognized, it becomes apparent that the desorption of most of these species is in fact totally controlled by the behaviour of water. The water-like species, desorbing from co-deposited mixtures, show only the single desorption coincident with water. The desorption behaviour of the water-like species can thus be described by scaling the desorption kinetics of water, which have already been measured in several studies (Haynes, Tro & George 1992; Speedy et al. 1996; Fraser et al. 2001), according to the relative concentration of the species. Similarly, the desorption of most of the intermediate species from a mixture with water is limited to the volcano desorption and co-desorption of trapped molecules. The ratio of the two peaks is determined by the thickness of the water film, and the

kinetics of the volcano peak is determined by the crystallization of the water. We have previously approximated the volcano desorption of CO in simulated TPD traces (Collings et al. 2003b). Only for the small intermediate species H_2S, C_2H_2 and C_2D_4, which exhibit limited diffusion through the water ice, will the desorption kinetics for molecules adsorbed to the ice surface be required for a complete description of their desorption behaviour. CH_4 and NO also require three sets of desorption kinetics to describe their monolayer, volcano and co-desorptions; however, due to their higher mobility in the ice, the monolayer desorption will have a much greater significance than for the small intermediate species. Multilayer desorption of CO, N_2 and O_2 from the ice surface was not observed in these experiments. However, the abundance of CO relative to water in interstellar ices is known to be frequently much higher than achieved with the exposures applied here. The CO concentration at which amorphous water ice formed at 10 K becomes saturated by CO diffusing into its porous structure from an external solid layer is yet to be experimentally measured. However, it is likely that at least in some astrophysical cases there is more than sufficient CO in the outer layer of van der Waals bonded (apolar) ice to saturate the inner layer of hydrogen bonded (polar) ice once diffusion has commenced. Although N_2 and O_2 are unlikely ever to be present in sufficient abundances to saturate the porous interstellar ice, they compete for the same adsorption sites as CO. Thus, multilayer desorption may be a significant process for N_2 and O_2 also, and the kinetics of all four desorption processes – multilayer, monolayer, volcano and co-desorptions – are required to describe desorption of CO, N_2 and O_2 fully in astrophysical environments.

The ice films that we produce by our various deposition procedures are somewhat crude models of dust-grain ice mantles. There are many factors that will influence the desorption characteristics of the various species that we have not considered. In these experiments, the concentration of each species with respect to water has been kept at roughly 5 per cent for consistency. This concentration overestimates the abundance of most of the species, but may underestimate the abundance of CO, CH_3OH, NH_3 and CO_2 in some cases. At higher concentrations, these species may start to affect the structure of the water-ice film, which in turn will affect the desorption characteristics of all species mixed with the water ice. These experiments have been performed on binary systems, and some deviation from the behaviour observed might be expected in multicomponent ices. For example, electron diffraction studies of H_2O–CH_3OH mixtures have demonstrated that the formation of CH_3OH clathrate hydrates is possible (Blake et al. 1991). The phase change associated with clathrate formation may induce a volcano desorption of other trapped species at a different temperature from that of water-ice crystallization. Variations in local concentrations within the ice mantles, due to processes such as segregation (Dartois et al. 1999), have not been considered, nor have the effects of other forms of energetic processing, such as cosmic ray bombardment and ultraviolet (UV) irradiation. Nevertheless, the results presented here show that treatment of the complex desorption processes of interstellar ice mantles can be dramatically simplified, since the behaviour of the water component of the ice mantles dominate the desorption kinetics of most species.

In previous desorption studies by Bar-Nun and coworkers, eight separate desorption processes were identified. In addition to multilayer, monolayer, volcano and co-desorption processes we have observed in this study, these authors describe (i) release of trapped gas at 35 $\sim$ 60 K during slow annealing, (ii) a further desorption in the $\sim$85–120 K range due to similar processes, (iii) desorption at 122 K possibly due to a glass transition in amorphous water ice, and (iv) a second volcano process at $\sim$150–160 K due to the conversion of cubic crystalline ice to hexagonal ice. The desorption traces were presented in these publications with a logarithmic scale on the *y*-axis which tends to exaggerate the significance of small desorption peaks. However, no evidence of any of these additional desorption processes was observed in the current study, even when the results were re-plotted with a logarithmic scale on the *y*-axis. The thickness of the ice films examined by Bar-Nun and coworkers ($\sim$2 microns) is an order of magnitude larger than those used in the current study. Given that the films we have studied are toward the upper limit of estimates of the thickness of ice mantles on interstellar dust grains, we suggest that the four additional desorption processes reported elsewhere are insignificant in desorption from interstellar dust grains.

It should be noted that the units of kelvin in the *x*-axes of Figs 1–3 denote actual temperature, rather than a measure of energy as is often the case in astrophysical publications. While the temperature of the desorption process is strongly dependent on the adsorption energy of the desorbing molecules, it is not directly proportional to the energy. Since desorption is a kinetic rather than equilibrium process, the desorption temperature is also influenced by the rate at which the ice is heated, and for non-first-order desorption processes such as multilayer desorption of ices, also on the thickness of the ice film. Therefore, the desorption temperatures measured under laboratory conditions cannot be transferred to astrochemical models. The rate of desorption is given by the expression

$$r_{\rm des} = \nu_i N^i \exp(-E_{\rm des}/RT) \quad (1)$$

where $r_{\rm des}$ is the desorption rate, $E_{\rm des}$ is the activation energy of the desorption process (adsorption energy) in units J mol^{-1}, i is the reaction order, N is the surface concentration of the desorbing species, T is the temperature, R is the gas constant, and ν_i is the order dependent pre-exponential constant. At the peak temperature, $T_{\rm p}$, the desorption rate is maximum such that $\mathrm{d}r_{\rm des}/\mathrm{d}t = 0$. Equation (1) can be rewritten

$$\frac{E_{\rm des}}{RT_{\rm p}^2} = \frac{\nu_i i N^{i-1}}{\beta} \exp\left(\frac{-E_{\rm des}}{RT_{\rm p}}\right) \quad (2)$$

where β is the heating rate, i.e. $\beta = \mathrm{d}T/\mathrm{d}t$. For a detailed mathematical description of desorption kinetics, see chapter 5 of Woodruff & Delchar (1986).

To illustrate the extent to which desorption temperatures will vary between laboratory and astrophysical conditions, we have created the series of simulations of water-ice desorption that are displayed in Fig. 4. These simulations have been produced applying the previously determined kinetics for water-ice desorption (Fraser et al. 2001) using a stochastic integration package,[1] and methods described in detail elsewhere (Ellis, Sidaway & McCoustra 1998; Collings et al. 2003b). The 100-L_m H_2O exposure used in all of the experiments described in this publication corresponds to an ice film of approximately 9.5×10^{17} molecules cm^{-2}. From published values of the density and porosity of water-ice vapour deposited at 10 K (Jenniskens & Blake 1994; Kimmel et al. 2001), an ice thickness of roughly 0.3 μm is estimated.

In Fig. 4(a), simulated TPD traces are presented for the desorption of a 0.3-μm ice film at heating rates ranging from 10 K s^{-1}, typical in many surface science experiments, to 1 K century^{-1}, approximating heating rates in hot cores (Viti & Williams 1999; Viti et al.

[1] Chemical Kinetics Simulator, Version 1.0, IBM Almaden Research Centre, 1995. Further information may be obtained from the CKS website at http://www.almaden.ibm.com/st/msim/ckspage.html

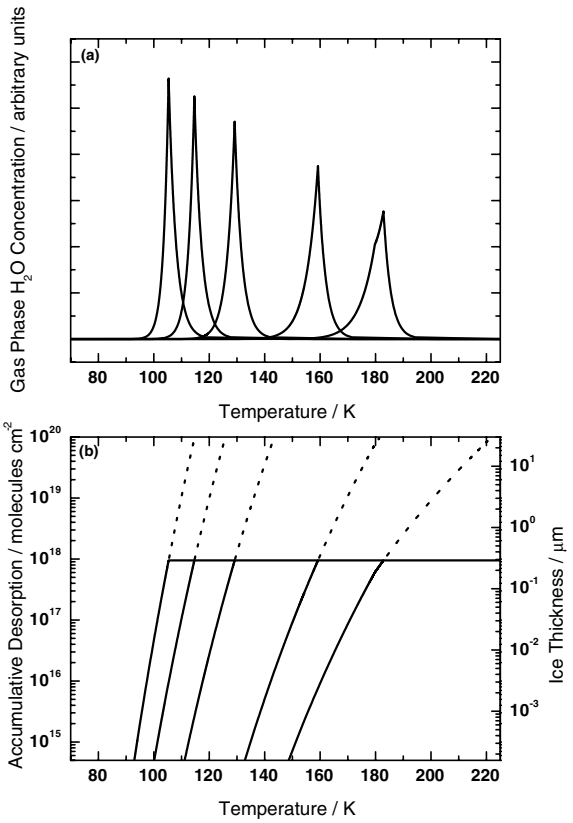

Figure 4. Simulated desorption profiles of water ice: reaction order, $i = 0$; pre-exponential factor, $\nu_0 = 10^{30}$; adsorption energy, $E_{\rm des} = 48$ kJ mol^{-1}; (a) TPD traces with heating rates and pumping speeds of, from left to right, 0.01 K yr^{-1} and 1.2×10^{-10} cm^2 molecule^{-1} s^{-1}, 1 K yr^{-1} and 1.2×10^{-8} cm^2 molecule^{-1} s^{-1}, 1 K d^{-1} and 4.3×10^{-6} cm^2 molecule^{-1} s^{-1}, 0.08 K s^{-1} and 0.03 cm^2 molecule^{-1} s^{-1}, 10 K s^{-1} and 3.75 cm^2 molecule^{-1} s^{-1}; (b) desorption to the gas phase with heating rates of, from left to right, 0.01 K yr^{-1}, 1 K yr^{-1}, 1 K d^{-1}, 0.08 K s^{-1} and 10 K s^{-1}: desorption up to 9.5×10^{17} molecules cm^{-2} (solid lines), desorption beyond 9.5×10^{17} molecules cm^{-2} (dotted lines).

2004), and including a simulation at our experimental heating rate of 0.08 K s^{-1}. The simulation is two-step process. Step 1 contains the zeroth-order kinetics of water-ice desorption, and step 2 contains the constant pumping rate of water vapour out of the experimental apparatus. In order for each simulation to produce a typical TPD 'peak', the pumping rate determined experimentally for the 0.08 K s^{-1} simulation has been scaled in proportion to the heating rate. The desorption temperature ranges from 183 K at a 10 K s^{-1} heating rate, to 105 K at 1 K century^{-1}.

Fig. 4(b) displays the results of the simulations if the pumping step is removed. Desorbed water molecules accumulate in the gas phase, therefore the simulation output is proportional to gas-phase concentration. The solid lines show the results for the simulations of the desorption of 0.3-μm water-ice film at the same heating rates as applied in Fig. 4(a). The temperatures at which the desorption is complete are equivalent for each heating rate to the peak temperatures in Fig. 4(a). A feature of zeroth-order desorption is that, for a given heating rate, the desorption profiles of varying thicknesses of ice can be overlaid. The dotted curves in Fig. 4(b) show, for each heating rate, the continuation of the desorption profile for ice films of thickness greater than 0.3 μm. Thus, it should be evident that the desorption temperature increases with increasing film thickness. Put simply, more ice takes longer to desorb, so a continually heated film will reach a higher temperature before desorption is complete. The accumulated desorption is thus also proportional to the film thickness, so a second *y*-axis can be added to the plot, allowing the desorption temperature of a given thickness of water ice to be read off at each of the heating rates. Note that in star formation the heating rate of the dust is dependent on the time taken for the star to reach the main sequence, and this is strongly dependent on the mass of the star (Viti & Williams 1999; Viti et al. 2004).

5 CONCLUSIONS

The desorption characteristics of a range of astrophysically relevant species during thermal processing of interstellar ice analogues have been studied using temperature programmed desorption. The behaviour of each species is complex; however, their treatment can be greatly simplified by separating the species into categories that can be modelled in the same manner. The water-like species, NH_3, CH_3OH and HCOOH, whose behaviour is dominated by hydrogen-bond interactions with water, have a single relevant co-desorption peak, and thus can be modelled with the known kinetics of water-ice desorption (Fraser et al. 2001) scaled according to their abundance relative to water. The CO-like species, N_2, O_2, CH_4 and NO (in addition to CO itself), have volcano desorption and co-desorption of trapped molecules, monolayer desorption from the surface of the water ice, and may also have a multilayer desorption if initially present with sufficient abundance in a layer separate from the water ice. These species can be approximately modelled using the same kinetics as determined for CO (Collings et al. 2003b) scaled according to abundance. Volcano and co-desorptions are the relevant processes for the remaining species, C_2D_4, C_2H_2, CO_2, OCS, CS_2, SO_2, CH_3CN and H_2S, which are classed as intermediate. Their desorption can be modelled using the appropriately scaled kinetics determined for the release of trapped CO (Collings et al. 2003b). For the smaller intermediate species C_2D_4, C_2H_2 and H_2S that have a limited ability to diffuse through porous water ice, a small monolayer desorption may also be relevant. Although the results presented provide a significant step in understanding the behaviour of ice mantles, we stress that they are preliminary in nature, and do not negate the need for more thorough laboratory studies of desorption from interstellar ice analogues. Nevertheless, the consequences of applying these data in modelling hot cores are very significant, and an exploration of this application is given in the accompanying article (Viti et al. 2004).

ACKNOWLEDGMENTS

This research was conducted with the support of the UK Particle Physics and Astronomy Research Council (PPARC) and the Leverhulme Trust. RC acknowledges the individual financial support of an Overseas Research Student (ORS) Award and the University of Nottingham, JWD acknowledges the individual financial support of a PPARC studentship, and SV acknowledges the individual financial support of a PPARC Advanced Fellowship. DAW is grateful for the award of the Leverhulme Trust Emeritus Fellowship. MAA was a final year undergraduate student at the time of his contribution to the research.

REFERENCES

Allamandola L. J., Bernstein M. P., Sandford S. A., Walker R. L., 1999, Space Sci. Rev., 90, 219

Ayotte P., Smith R. S., Stevenson K. P., Dohnálek Z., Kimmel G. A., Kay B. D., 2001, J. Geophys. Res., 106, 33387
Bar-Nun A., Herman G., Laufer D., Rappaport M. L., 1985, Icarus, 63, 317
Blake D., Allamandola L., Sandford S., Hudgins D., Freund F., 1991, Sci, 254, 548
Collings M. P., Dever J. W., Fraser H. J., McCoustra M. R. S., 2002, NASA/CP-2002-21186, 192
Collings M. P., Dever J. W., Fraser H. J., McCoustra M. R. S., Williams D. A., 2003a, ApJ, 583, 1058
Collings M. P., Dever J. W., Fraser H. J., McCoustra M. R. S., 2003b, Ap&SS, 385, 633
Dartois E., Demyk K., d'Hendecourt L., Ehrenfreund P., 1999, A&A, 351, 1066
Dohnálek Z., Kimmel G. A., Joyce S. A., Ayotte P., Smith R. S., Kay B. D., 2001, J. Phys. Chem. B, 105, 3747
Ellis G., Sidaway J., McCoustra M. R. S., 1998, J. Chem. Soc. Faraday Trans., 94, 2633
Fraser H. J., Collings M. P., McCoustra M. R. S., Williams D. A., 2001, MNRAS, 327, 1165
Fraser H. J., Collings M. P., McCoustra M. R. S., 2002, Rev. Sci. Instr., 73, 2161
Haynes D. R., Tro N. J., George S. M., 1992, J. Phys. Chem., 96, 8502
Hofner P., Wiesemeyer H., Henning T., 2001, ApJ, 549, 425
Horimoto N., Kato H. S., Kawai M., 2002, J. Chem. Phys., 116, 4375
Hudson R. L., Donn B., 1991, Icarus, 94, 326
Jenniskens P., Blake D. F., 1994, Sci, 265, 753
Jones A. P., Williams D. A., 1984, MNRAS, 290, 955
Jørgensen J. K., Schöier F. L., van Dishoeck E. F., 2002, A&A, 389, 908
Kimmel G. A., Dohnálek Z., Stevenson K. P., Smith R. S., Kay B. D., 2001, J. Chem. Phys., 114, 5295
Kouchi A., 1990, J. Cryst. Growth, 99, 1220
Laufer D., Kochavi E., Bar-Nun A., 1987, Phys. Rev. B, 36, 9219
Nomura H., Millar T. J., 2004, A&A, 414, 409
Notesco G., Bar-Nun A., 1996, Icarus, 122, 118
Notesco G., Bar-Nun A., Owen T., 2003, Icarus, 162, 183
O'Neill P. T., Williams D. A., 1999, Ap&SS, 266, 539
Palumbo M. E., Geballe T. R., Tielens A. G. G. M., 1997, ApJ, 479, 839
Pratap P., Megeath S. T., Bergin E. A., 1999, ApJ, 517, 799
Ramseyer C., Giradet C., Bartolucci F., Schmitz G., Francy R., Teillet-Billy D., Gauyacq J. P., 1998, Phys. Rev. B, 58, 4111
Sandford S. A., Allamandola L. J., Tielens A. G. G. M., Valero G. J., 1988, ApJ, 329, 498
Sandford S. A., Allamandola L. J., 1988, Icarus, 76, 201
Sandford S. A., Allamandola L. J., 1990, ApJ, 355, 357
Schöier F. L., Jørgensen J. K., van Dishoeck E. F., Blake G. A., 2002, A&A, 390, 1001
Schmitt B., Grim R. J. A., Greenberg J. M., 1988, in Bailey M. E., Williams D. A., eds, Proc. Dust in the Universe. Manchester, 1987. Cambridge Univ. Press, Cambridge, p. 291
Schmitt B., Greenberg J. M., Grim R. J. A., 1989, ApJ, 340, L33
Smith R. S., Huang C., Wong E. K. L., Kay B. D., 1997, Phys. Rev. Lett., 79, 909
Speedy R. J., Debenedetti P. G., Smith R. S., Huang C., Kay B. D., 1996, J. Chem. Phys., 105, 240
Viti S., Williams D. A., 1999, MNRAS, 305, 755
Viti S., Collings M. P., Dever J. W., McCoustra M. R. S., Williams D. A., 2004, MNRAS, in pres (Paper II, this issue)
Woodruff D. P., Delchar T. A., 1986, Modern Techniques of Surface Science. Cambridge Univ. Press, Cambridge
Yoshinobu J., Kawai M., 1996, Surf. Sci., 368, 247

This paper has been typeset from a Microsoft Word file prepared by the author.